DEPOSITION OF INHALED MONODISPERSE AEROSOLS IN SMALL RODENTS

OTTO G. RAAB*, HSU-CHI YEH, GEORGE J. NEWTON,
ROBERT F. PHALEN† and DAVID J. VELASQUEZ

Inhalation Toxicology Research Institute,
Lovelace Foundation, Albuquerque, N.M., U.S.A.

Abstract—Aerosols of five different sizes varying from about 0.05 μm to 3 μm in aerodynamic equivalent diameter were prepared from spherical aluminosilicate particles ($\rho = 2.2$ g/cm^3) labelled with ^{169}Yb. Fifty hamsters and fifty rats were exposed, while anaesthetized, to these monodisperse aerosols under controlled laboratory conditions to determine quantitatively deposition in the respiratory airways with respect to particle size and volume of air inhaled. Ten animals of each species were exposed to each of the particle sizes. Five animals were exposed simultaneously for 20 min in an inhalation exposure apparatus which provided automatic recordings of respiratory rates and volumes using individual whole-body plethysmographs; three were sacrificed immediately after exposure and the remaining two after 20 h had elapsed for radioanalysis of selected tissues to determine deposition quantities and organ distribution. Detailed results are given for the observed deposition fractions for the different aerosols in the various parts of the respiratory tract. The lowest fractional total deposition occurred for particles between 0.5 μm and 1 μm in aerodynamic equivalent diameter. Relative deposition among the various lung lobes showed remarkable consistency with respect to particle size. Based upon the results of morphometric measurements of replica casts of lungs of the two species, interpretations are made relating the observed deposition phenomena to tracheobronchial anatomy.

INTRODUCTION

Many investigators use rodents of various types including rats and Syrian hamsters in inhalation toxicity studies with polydisperse aerosols. THOMAS (1969) reported results of detailed deposition studies of the exposure of mice, rats and guinea pigs to various polydisperse aerosols. In such studies the deposition and clearance of the particles in the respiratory tract and the pattern of insult and resulting biological effects may vary markedly for particles of different sizes. These variations are difficult to sort out and evaluate with data from polydisperse aerosols where particles of widely different sizes are present. With the availability of carefully prepared and characterized

* Current address: Radiobiology Laboratory, School of Veterinary Medicine, University of California, Davis, California, U.S.A.

† Current address: Department of Community and Environmental Medicine, University of California, Irvine, California, U.S.A.

monodisperse aerosols of insoluble forms labelled with radionuclides, the behaviour of specific sizes of particles can be studied. Although some studies have been performed with rodents and monodisperse aerosols, such as those reported by HOLMA (1968), these were limited in scope and involved only larger particles.

In the research reported herein, a detailed investigation was conducted of the deposition of well characterized monodisperse aerosols of aluminosilicate spheres labelled with ^{169}Yb. The respiratory parameters describing the breathing of each animal during each exposure were carefully measured and recorded. By measurement of the radiolabel in various parts of the respiratory tract and other organs it was possible to determine the fractional deposition in the major regions of the respiratory tract of each particle size for each animal. Morphometric measurements of replica casts of the respiratory airways of the lungs of each species were made to provide data on the typical path characteristics for each lung lobe for evaluation of the effects of airway geometry on deposition phenomena.

The results of these studies help clarify the effects of particle size on regional deposition and interlobar deposition of inhaled particles in rodents. The particle size providing a minimized fraction of bronchial deposition was observed to be about 0.5μm aerodynamic equivalent diameter. The effect of particle size on lobar deposition was found to be consistent with the airway morphometry of the different lobes.

MATERIALS AND METHODS

Basic Considerations

The assumed practical definition of a monodisperse particle size distribution is a distribution of particles whose coefficient of variation (ratio of standard deviation to the mean) is less than 0.2 (20%) as recommended by FUCHS and SUTUGIN (1966). For a size distribution which is adequately described by a log-normal function, this is about equivalent to a geometric standard deviation $\sigma_g < 1.2$. It is tacitly assumed in this definition that a monodisperse aerosol consists of particles of relatively uniform composition and physical density.

The sizes of spherical particles as used in this study can be described either by their geometric diameter, D, or with an aerodynamic size. For calibration of inertial samplers the aerodynamic resistance diameter, D_{ar}, given by RAABE (1975) was used with:

$$D_{ar} = D\sqrt{[\rho C(D)]} \tag{1}$$

for spherical particles of diameter D with ρ the dimensionless specific gravity of a particle exactly equal numerically to the physical density in g/cm^3 and $C(D)$ the slip correction used to correct Stokes' Law for the behaviour of small particles.

The TASK GROUP ON LUNG DYNAMICS (1966) has recommended an aerodynamic (equivalent) diameter for use in inhalation studies defined as the "diameter of a unit density sphere with the same settling velocity as the particle in question". Hence the unit density aerodynamic (equivalent) diameter, D_{ae}, is given by:

$$D_{ae} = D_{ar}/\sqrt{C(D_{ae})} \tag{2}$$

with $C(D_{ae})$ the slip correction for a particle of geometric diameter equal to D_{ae}. For D_{ae} values greater than 0.3 μm corresponding D_{ar} values are about 0.1μm larger.

Preparation of Aerosols

The monodisperse aerosols used in these studies were prepared by separating and collecting monodisperse fractions of a polydisperse aerosol of fused aluminosilicate spheres which were labelled with ^{169}Yb, a radioactive isotope of ytterbium. The polydisperse aerosol was prepared as described by RAABE *et al.* (1971). Basically this procedure consisted of treating montmorillonite clay samples with concentrated H_2O_2 to degrade organic impurities, decanting the finely-divided clay suspension,

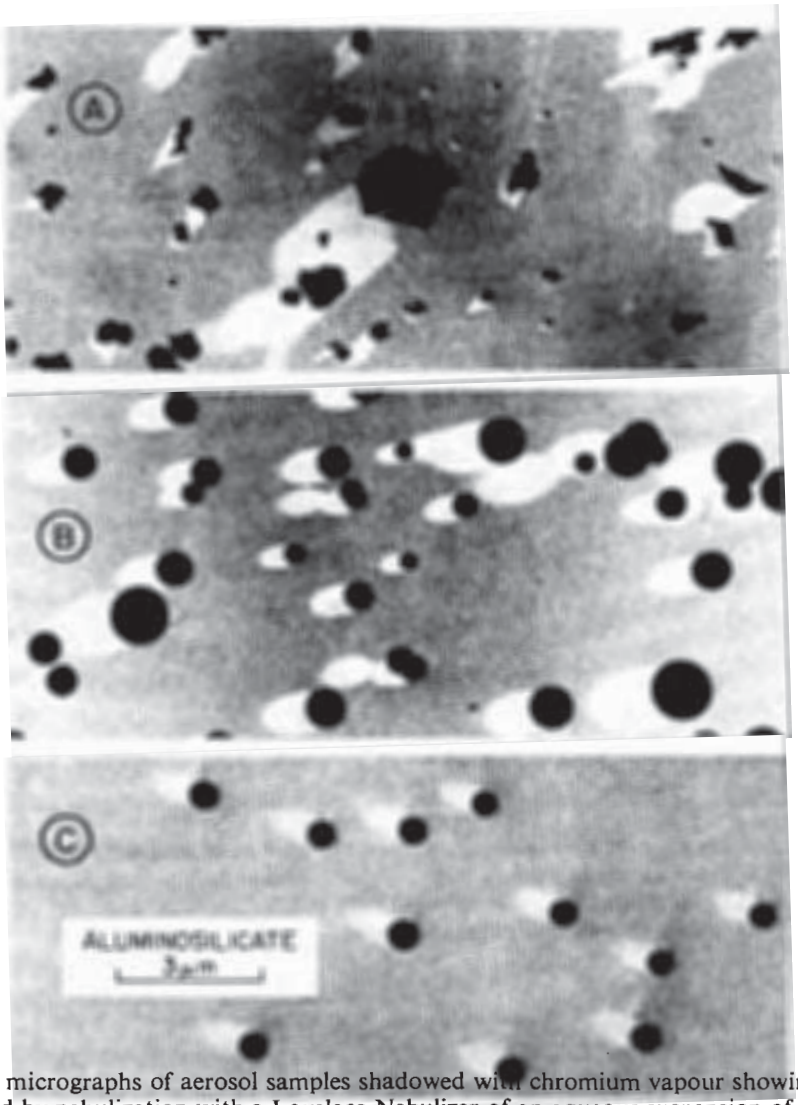

FIG. 1. Electron micrographs of aerosol samples shadowed with chromium vapour showing (A) aerosol generated by nebulization with a Lovelace Nebulizer of an aqueous suspension of montmorillonite clay, (B) aerosol of aluminosilicate spheres created by heating of the clay aerosol to 1150°C and (C) monodisperse particles collected with the spiral duct centrifuge used to prepare monodisperse aerosols for inhalation studies.

treatment with sodium chloride solution to load the ion-exchange sites with sodium cations, dialysis with deionized water to remove excess sodium chloride and mixing $^{169}YbCl_3$ with the final clay suspension to allow for ion exchange of ^{169}Yb cations into the clay. The resulting suspension of ^{169}Yb-labelled clay was filtered and washed with deionized water to remove unexchanged ^{169}Yb. The polydisperse aerosol (Fig. 1A) was generated by nebulization of an aqueous suspension of 10 mg clay per ml and passed through a quartz tube furnace at 1150°C to fuse the clay particles into aluminosilicate spheres (Fig. 1B) in which the ^{169}Yb label was entrapped.

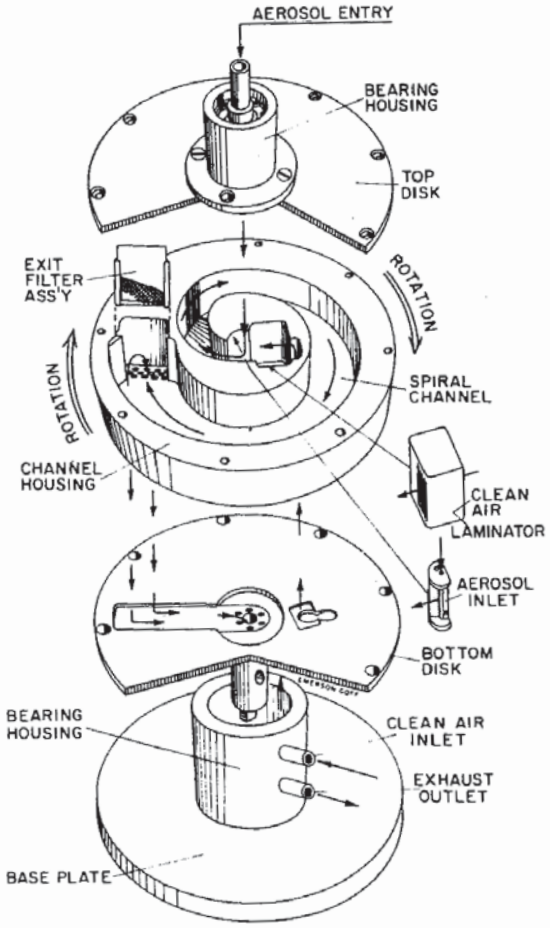

FIG. 2. Schematic drawing of an exploded view of the Lovelace Aerosol Particle Separator (LAPS), the spiral duct centrifuge used in this study to separate and collect monodisperse size fractions of fused aluminosilicate particles labelled with ^{169}Yb (from KOTRAPPA *et al.*, 1972, by permission of Pergamon Press Ltd., Oxford).

This ^{169}Yb-labelled aluminosilicate aerosol was sampled with a Lovelace Aerosol Particle Separator, LAPS (KOTRAPPA and LIGHT, 1972), a spiral duct aerosol centrifuge (STÖBER and FLACHSBART, 1969), which operates as an aerosol spectrometer (Fig. 2). Aerosols drawn into the LAPS are separated and collected according to their aerodynamic properties under the influence of centrifugal and coriolis forces as the duct rotor is spun at a constant 60 Hz with an induction motor. The aerosol sample (0.3 l./min) is drawn into the spiral duct through an inlet slit at the axis of the rotor and

flows parallel to a laminar stream of clean air (4.7 l./min). The aerosol particles move to the outer wall of the duct with speeds depending upon their respective aerodynamic diameters and deposit upon a 46.2 cm long, 3.1 cm high and 0.01 cm thick stainless-steel foil lining the outer wall of the spiral duct. Particles with aerodynamic (resistance) diameters, D_{ar}, larger than 0.6 μm are collected on the foil and the smaller particles are collected on a 3 × 3 cm glass fibre filter at the end of the LAPS duct. After collection of a suitable quantity of particles with the LAPS, the foil was removed and cut into twenty-three segments providing different size groups of monodisperse particles which were subsequently suspended in water for nebulization to yield the desired monodisperse aerosols for the inhalation exposures.

The basic idea of aerodynamically separating insoluble particles into monodisperse size groups using a spiral duct aerosol centrifuge and subsequently generating monodisperse aerosols from these separated particles was suggested by KOTRAPPA and MOSS (1971). The equipment and methods used in this study were essentially as described by RAABE *et al.* (1975) and NEWTON *et al.* (1976).

Figure 3 shows the D_{ar} calibration of the LAPS, which was performed using polystyrene latex particles (Dow Diagnostics, Indianapolis, Indiana, U.S.A.), the equivalent geometric size of the clay aluminosilicate particles (ρ = 2.2 g/cm^3) used in this study,

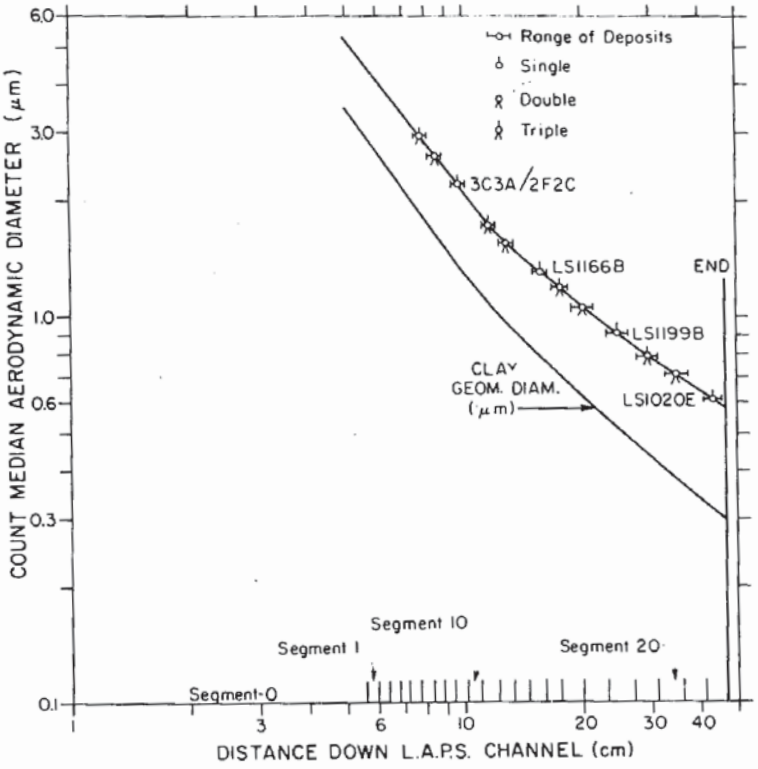

FIG. 3. Calibration for the Lovelace Aerosol Particle Separator (LAPS) used to separate and collect aluminosilicate particles into monodisperse fractions showing the count median aerodynamic (resistance) diameter, D_{ar}, versus the position on the collection foil given by the distance down channel. The data is based upon singlets, doublets and triplets of various latex aerosols indicated by the manufacturer's identification numbers. Also shown is a curve indicating the geometric diameter of fused clay aluminosilicate particles (ρ = 2.2 g/cm^3) collected in the separator.

and the positions of the twenty-three segments of the collection foil. Figure 1C is an electronmicrograph showing a sample shadowed with chromium vapour of one size of monodisperse aluminosilicate particles.

Monodisperse sizes used in this study had aerodynamic (resistance) diameters, D_{ar}, of 3.15 μm, 2.19 μm, 1.14 μm and 0.61 μm which corresponded to aerodynamic (equivalent) diameters, D_{ae}, of 3.05 μm, 2.09 μm, 1.04 μm and 0.52 μm, respectively, at the local conditions (21°C, barometric pressure 83 kPa). These aerosols were generated by nebulization of dilute aqueous suspensions with the concentration chosen to provide an aerosol with a suitably high proportion of single particles as opposed to aggregates that are formed when two or more monodisperse particles are aerosolized in the same droplet from the nebulizer. RAABE (1968) provided the criteria by which these concentrations were determined. The pH of each suspension was adjusted to 10 with NH_3 gas for stabilization. The Lovelace nebulizer (RAABE, 1970) was used to generate these aerosols for the exposures; it provided about 50μl of droplets in 1.5 l./min of air with volume median diameter of about 5.8 μm ($\sigma_g = 1.8$). Each aerosol was mixed with about 10 l./min of clean, dry air to dry the droplets and passed through a 2 mCi ^{85}Kr discharger (Thermo Systems, St Paul, Minn.) to reduce the aerosol particle charge distribution to Boltzmann equilibrium prior to inhalation by the animals.

In addition to the four monodisperse aerosols, a fifth aerosol of smaller particles was prepared which turned out to be two slightly different near monodisperse aerosols ($\sigma_g = 1.5$) with activity median diameter about 0.3 μm D_{ar} (0.2 μm D_{ae}) in one case and about 0.1 μm D_{ar} (0.05 μm D_{ae}) in the other. These were generated by nebulization of dilute silicic acid solutions with ^{169}Yb and conversion to silicate particles by heat treatment at 1150°C. When required, these smaller particles were delivered directly to the exposure apparatus without intermediate LAPS separation; the ^{85}Kr discharger was used.

Use of ^{169}Yb

The ^{169}Yb label used in this study was entrapped in the insoluble fused aluminosilicate particles and its radioactive emissions were used for quantitative measurement of the aerosol concentration and regional deposition in the animals. The ^{169}Yb decays by electron capture with a half-life of 31.3 days. It emits a host of highly detectable gamma and X-ray photons including 310 keV and 200 keV gamma photons in 11 and 49%, respectively, of the disintegrations. It is available with specific activities exceeding 1000 Ci/g (General Electric Co., Vallecitos, California).

Aerosol samples were assayed using a NaI crystal and multichannel analyser. Tissue samples were assayed using large volume liquid scintillation well counters (Packard Instrument Co., Inc., Downers Grove, Illinois) and, in addition, the smaller organ samples were assayed with a NaI auto-gamma counter (Nuclear-Chicago, Inc., Chicago, Illinois).

Exposure Apparatus and Procedures

Syrian hamsters and rats were exposed individually in the five-port inhalation exposure apparatus with associated whole-body plethysmographs which was described by THOMAS and LIE (1963). A sixth port in the apparatus was used for obtaining

aerosol samples including seven-stage cascade impactor samples (MERCER *et al.*, 1970) for verification of the size and monodispersity of the aerosols, filter samples for measurement of ^{169}Yb concentration during the exposure and electrostatic precipitator samples (MORROW and MERCER, 1964) for electron microscopic evaluation of the aerosols. Figure 4 is a schematic drawing of the exposure system used in this study; components were housed in three stainless-steel and glass glove boxes for radiological safety. Each plethysmograph had one animal in an airtight plastic chamber with the head protruding through an airtight latex rubber collar. In this apparatus the aerosol was drawn continuously past each animal's head. Pressure changes in the plethysmo-

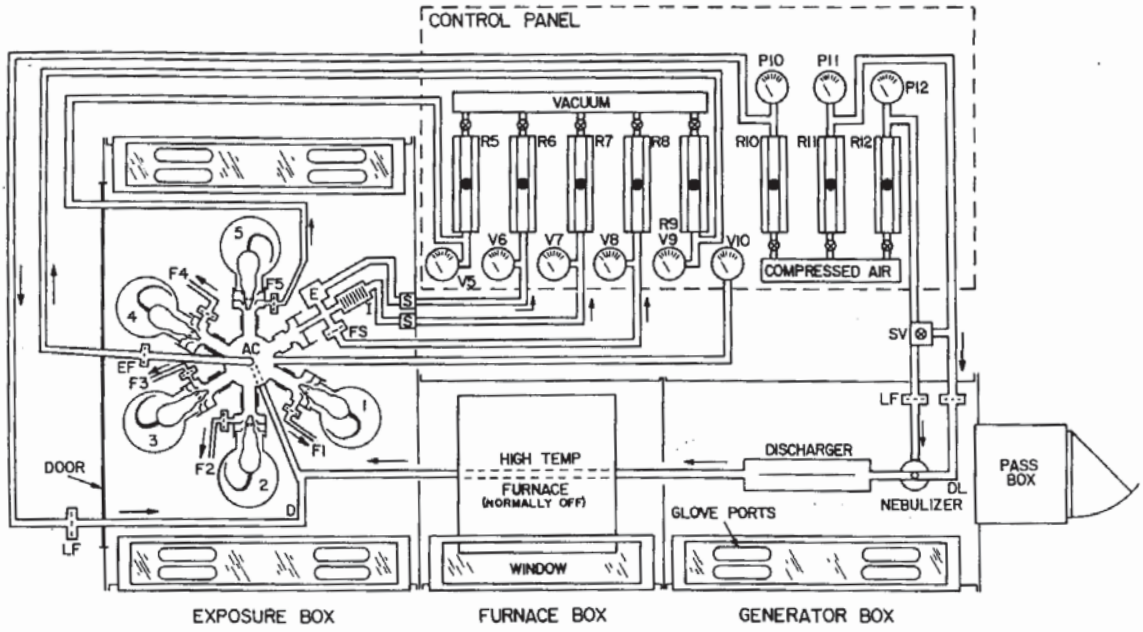

FIG. 4. Schematic representation of the apparatus used in this study for simultaneous inhalation exposure of five rodents to monodisperse aerosols of ^{169}Yb-labelled fused aluminosilicate particles. Each animal is in a separate whole-body plethysmograph. Also shown are the three stainless-steel glove boxes enclosing the equipment and the associated controls. Each monodisperse suspension of aluminosilicate spheres was aerosolized with the nebulizer operated by compressed air (filtered by line filter, LF) supplied and metered via rotameter R12 at a pressure given by gauge P12 when solenoid valve SV is actuated. The aerosol was first diluted (to provide for droplet evaporation) with air passing through DL via a filter and rotameter R11 at pressure indicated by gauge P11. When solenoid valve SV was not actuated, the air which normally passed through the nebulizer was directed to the diluting air line via a valve at SV (which had been adjusted to provide a flow equal in volumetric rate to the normal nebulizer output rate). The aerosol passed through a discharger warmed to 40°C to enhance droplet evaporation and having a sealed radioactive source (^{85}Kr) which reduced the electrostatic charge distribution to Boltzmann equilibrium. The aerosol passed next through a tube furnace (not used, at ambient temperature) and was mixed with additional diluting air at D supplied via line filter LF and rotameter R10 at pressure given by P10. The aerosol then passed into the aerosol chamber, AC, and a portion was drawn past the head of each of the five animals (in plethysmographs 1–5) at flow rates controlled by rotameters R1–R4 (not shown) and R5 (shown) at pressure given by vacuum gauges V1–V4 (not shown) and V5 (shown), respectively. Samples taken included filter sample FS, electrostatic precipitator sample E, cascade impactor sample I, and exhaust filter EF metered via rotameters R6–R9, respectively, at pressures indicated by vacuum gauges V6–V9, respectively. The pressure in the aerosol chamber (normally −250 Pa) was indicated by vacuum gauge V10. The aerosol of smallest particles was generated from dilute silicic acid solutions (with ^{169}Yb) with the high-temperature furnace at 1150°C. Normal conditions: 21°C and 50% relative humidity.

graph chamber were used to monitor respiratory activity. Such respiratory data were both plotted on a strip chart for analysis by hand and recorded on magnetic tape for analysis by analogue computer to determine tidal volumes, minute volumes and breathing rates.

Prior to exposure, each animal was anaesthetized with sodium pentobarbital given intraperitoneally to render it unconscious for about 1 h. In a few cases, individual animals succumbed to the anaesthetic and were not considered in analyses of the results. Each animal was then placed in a plethysmograph unit, a leak test was made and the front of the plethysmograph chamber was inserted into an exposure port. The exposure began after all chambers were inserted. Exposures were normally 20 min in duration.

The Syrian hamsters used in this study were non-inbred golden Syrian hamsters, *Mesocricetus auratus*, Sch: (SYR) obtained from ARS/Sprague Dawley, Madison, Wisconsin, U.S.A. The black and white hooded rats used in this study were Long Evans black and white hooded rats, *Rattus norvegicus*, Blu: (LE)BR obtained from Black Spruce Farms Inc., Altamont, New York, U.S.A. Ten Long Evans black and white rats and ten golden Syrian hamsters were exposed to each of the five particle sizes, four monodisperse and one near monodisperse. In all, fifty animals of each species were exposed. Each sex was represented by half of the animals exposed to each aerosol. Twenty separate exposures of five animals each were conducted. For each exposure three animals were immediately sacrificed and dissected for radioassay of the tissues and two were placed in excreta-collection cages to be sacrificed 20 h after the exposure. Each animal was carefully dissected after sacrifice and tissue samples were placed in preweighed containers for weighing and radiation counting. The individual tissue samples for each animal were (a) right apical lobe of lung, R.A.; (b) right cardiac lobe of lung, R.C.; (c) right diaphragmatic lobe of lung, R.D.; (d) right intermediate lobe of lung, R.I.; (e) complete left lung (both left apical, L.A., and left diaphragmatic, L.D., lobes); (f) trachea below larynx including carina and portion of major bronchi; (g) larynx and associated tissue; (h) skull; (i) G.I. tract; (j) pelt; (k) paws and tail; (l) carcass including spleen and kidney; (m) liver; (n) head skin and (o) miscellaneous remainder including paper towels and dissection wipes. Excreta samples were also counted for animals sacrificed 20 h after exposure.

Deposition data for the lung lobes of the immediate sacrifice and 20 h sacrifice animals were compared for each aerosol particle size to evaluate the lung clearance that occurred during the first 20 h after exposure. Material cleared from the lung during these 20 h was assumed to have been deposited on the ciliated airways of the bronchial region, and the remainder was assumed to be pulmonary deposit. The fraction, f_T, of the total respiratory tract deposit which was represented by the bronchial deposit is given on the average by:

$$f_T = \left(\frac{L_0}{T_0}\right)_{\text{avg}} - \left(\frac{L_{20}}{T_{20}}\right)_{\text{avg}} \tag{3}$$

with L_0 and L_{20} the observed lung burdens of deposited aerosol and T_0 and T_{20} the total respiratory tract deposition in the immediate and 20 h sacrifice animals, respectively, and $(\ )_{\text{avg}}$ indicating the average for all animals; T_{20} includes all observed internally deposited activity including excreta and is equivalent to T_0. The fraction,

TABLE 1. LOBAR WEIGHT DISTRIBUTIONS FOR BLACK AND WHITE HOODED RAT AND SYRIAN HAMSTER

Species	Black and white hooded rat						Syrian hamster					
Number and sex	30—Male			28—Female			27—Male			27—Female		
	Mean	S.D.	%T.L.	Mean	S.D.	%T.L.	Mean	S.D.	%T.L.	Mean	S.D.	%T.L.
Body weight (g)	464	36		257	17		132	13		136	15	
Age (days)	114	12		114	12		148	30		149	33	
Right apical (g)	0.230	0.085	10.6	0.152	0.032	10.2	0.0827	0.012	10.8	0.105	0.030	11.2
Right cardiac (g)	0.296	0.070	13.7	0.211	0.047	14.2	0.0966	0.039	12.6	0.115	0.035	12.3
Right diaphragmatic (g)	0.624	0.126	28.9	0.427	0.083	28.7	0.233	0.038	30.5	0.283	0.060	30.1
Right intermediate (g)	0.252	0.060	11.7	0.186	0.039	12.5	0.0859	0.025	11.2	0.114	0.031	12.1
Left lung (both lobes) (g)	0.760	0.152	35.2	0.514	0.092	34.5	0.266	0.053	34.8	0.322	0.088	34.3
Total (g)	2.162			1.490			0.764			0.939		
Breaths/min*	78	24		58	19		69	36		49	24	
Minute volume (ml)*	207	85		111	43		45	22		40	20	

* For anaesthetized animals at room temperature and pressure (21° C, 83 kPa).

f_L, of the initial lung burden which is represented by the bronchial deposit is given on the average by:

$$f_L = f_T \left(\frac{T_0}{L_0}\right)_{\text{avg}}$$

Airway Morphometry

Replica casts of lungs of rats and hamsters were carefully prepared and morphometric measurements made. Silicone-rubber castings were made in lungs that were intact and still within the thorax by an *in situ* method that has been described by PHALEN *et al.* (1973). After the injected rubber had cured, the lungs were removed from the thorax, and the lung tissues were digested in sodium hydroxide. Each flexible replica was carefully trimmed to leave only that portion of the tracheobronchial tree down to and including terminal bronchioles. Measurements on casts, performed by five trained persons, included branching angles, lengths, diameters and inclinations to gravity for individual bronchial tubes. Morphometry was performed on casts from one rat and one hamster. A "typical path" model of the tracheobronchial airways down to and including terminal bronchioles was developed for each lobe from computer analyses of the morphometric data to provide a simple scheme for relating morphometry to particle deposition phenomena.

RESULTS

Anatomical and Physiological Data

Basic characteristics of the animals used in this study (and some extras) are summarized in Table 1, including the averages and standard deviations for body weight, age and lung lobe weights at necropsy. Although the absolute weights of each lobe varied among species and sexes, their relative weights expressed as percent of total lung weight were nearly the same irrespective of sex and species. This property simplified the interpretation of relative deposition in each lung lobe.

Deposition Data

The values of f_T and f_L and the calculated standard errors observed in this study for both hamsters and rats are given as percentages in Table 2 for the various particle

TABLE 2. BRONCHIAL (20-H CLEARED) DEPOSITION AS PERCENTAGE OF INITIAL TOTAL DEPOSIT IN RESPIRATORY TRACT, f_T, AND AS PERCENTAGE OF INITIAL LUNG BURDEN, f_L (WITH CALCULATED STANDARD ERRORS), WITH RESPECT TO AEROSOL AERODYNAMIC EQUIVALENT DIAMETER

		Aerodynamic diameter (μm) D_{ae}				
		$\leqslant 0.2$	0.52	1.04	2.09	3.05
Hamster	f_T	27 ± 2	5 ± 7	18 ± 9	16 ± 7	6 ± 7
	f_L	37 ± 2	6 ± 9	34 ± 15	58 ± 15	28 ± 28
Rat	f_T	20 ± 3	4 ± 2	15 ± 8	5 ± 8	10 ± 5
	f_L	24 ± 4	5 ± 3	24 ± 13	18 ± 31	51 ± 23

sizes. Although quite variable, they show basic trends with the bronchial fractions being minimum for the 0.52 μm particles.

Using the calculated average values of f_L and f_T, the observed lung burdens of ^{169}Yb were divided into appropriate bronchial and pulmonary portions. Each deposition quantity was converted to the fraction of the total inhaled aerosol which was associated with that quantity by dividing by the product of animal minute volume, the exposure time and the aerosol concentration. The skull and gastrointestinal activity for the immediate sacrifice animals was taken to represent the nasopharyngeal deposit. The results are summarized in Table 3. Other internal organs were free of ^{169}Yb.

TABLE 3. MEAN DEPOSITION PERCENTAGES AND OBSERVED STANDARD ERRORS OF INHALED MONODISPERSE ^{169}Yb-LABELLED ALUMINOSILICATE AEROSOLS

	Aerodynamic diameter (μm) D_{ae} (equivalent unit density sphere)				
	$\leqslant$ 0.2	0.52	1.04	2.09	3.05
HAMSTERS					
Lung — Pulmonary	13.2 ± 1.9	12.4 ± 1.7	5.5 ± 0.7	5.5 ± 1.3	9.6 ± 2.3
Lung — Bronchial	7.9 ± 1.1	0.85 ± 0.09	3.0 ± 0.4	7.9 ± 0.7	3.4 ± 0.2
Trachea	0.3 ± 0.1	0.10 ± 0.03	0.09 ± 0.02	0.4 ± 0.1	0.6 ± 0.3
Larynx	0.9 ± 0.4	0.2 ± 0.1	1.0 ± 0.5	4.2 ± 2.9	4.2 ± 1.8
Naso-pharynx — Skull	6.9 ± 1.1	2.7 ± 0.3	4.6 ± 0.8	24.1 ± 5.5	22.6 ± 5.5
Naso-pharynx — G.I.	0.3 ± 0.1	0.7 ± 0.3	0.3 ± 0.1	0.5 ± 0.2	15.9 ± 6.6
Total of above values	29.5 ± 2.5	16.9 ± 1.8	14.5 ± 1.2	42.6 ± 6.4	56.3 ± 9.1
Total (observed)	28.2 ± 4.0	17.0 ± 1.8	16.5 ± 2.1	49.3 ± 4.7	56.0 ± 2.8
RATS					
Lung — Pulmonary	20.7 ± 1.7	10.7 ± 1.3	6.6 ± 0.9	7.9 ± 1.9	4.9 ± 0.9
Lung — Bronchial	6.3 ± 0.5	0.61 ± 0.07	2.1 ± 0.3	1.9 ± 0.3	5.2 ± 0.4
Trachea	0.6 ± 0.1	0.2 ± 0.1	0.02 ± 0.01	0.09 ± 0.04	0.2 ± 0.1
Larynx	0.07 ± 0.04	0.2 ± 0.1	0.2 ± 0.2	0.7 ± 0.5	3.4 ± 0.06
Naso-pharynx — Skull	4.5 ± 0.6	2.0 ± 0.4	4.5 ± 0.8	17.9 ± 4.5	17.5 ± 2.8
Naso-pharynx — G.I.	0.1 ± 0.1	0.3 ± 0.1	0.8 ± 0.6	0.04 ± 0.03	17.3 ± 6.6
Total of above values	32.3 ± 1.9	14.0 ± 1.4	14.0 ± 1.4	28.5 ± 4.9	48.5 ± 7.2
Total (observed)	31.8 ± 2.6	14.1 ± 1.7	14.2 ± 1.7	41.1 ± 6.8	52.8 ± 3.8

Tables 4 and 5 show the relative lobar burdens of the immediate (0-h) and 20-h sacrifice rats, respectively; and Tables 6 and 7 show the immediate and 20-h burdens, respectively, for the hamsters. Comparison of the data for the two sacrifice times for each species shows that the relative amounts in the lobes varies little up to 20 h post-exposure. This implies that clearance rates were about the same for all lobes.

TABLE 4. RELATIVE LOBAR DEPOSITION OF ^{169}Yb LABELLED ALUMINOSILICATE AEROSOLS IN BLACK AND WHITE HOODED RATS AT 0-H POST-EXPOSURE. PERCENT OF TOTAL LUNG BURDEN (mean and standard deviation)

	Aerodynamic diameter (μm) D_{ae} (equivalent unit density sphere)					
Lobe	3.05(5)*	2.09(4)	1.04(7)	0.52(6)	$\leqslant$ 0.2(6)	Av.(28)
R.A.	13.77 ± 2.33	14.77 ± 3.52	11.41 ± 1.73	11.35 ± 1.13	10.95 ± 1.73	12.20
R.C.	12.07 ± 5.06	12.27 ± 0.64	14.19 ± 1.31	14.17 ± 1.97	13.23 ± 1.49	13.35
R.D.	25.86 ± 8.42	28.84 ± 3.22	28.19 ± 2.17	25.23 ± 2.77	26.99 ± 1.56	26.98
R.I.	10.44 ± 2.64	10.31 ± 1.76	11.31 ± 0.89	12.42 ± 1.14	12.68 ± 1.49	11.54
Left lung	37.98 ± 5.19	33.82 ± 2.48	34.80 ± 2.41	36.83 ± 2.17	36.15 ± 1.81	35.95

* Number of animals in parenthesis.

TABLE 5. RELATIVE LOBAR DEPOSITION OF ^{169}Yb LABELLED ALUMINOSILICATE AEROSOLS IN BLACK AND WHITE HOODED RATS AT 20-H POST-EXPOSURE. PERCENT OF TOTAL LUNG BURDEN (mean and standard deviation)

	Aerodynamic diameter (μm) D_{ae} (equivalent unit density sphere)					
Lobe	3.05(4)*	2.09(4)	1.04(3)	0.52(4)	$\leqslant$ 0.2(4)	Av.(19)
R.A.	11.23 ± 4.91	12.79 ± 1.88	12.45 ± 1.03	10.45 ± 0.53	12.21 ± 1.97	11.79
R.C.	14.12 ± 2.96	14.29 ± 1.20	12.79 ± 3.04	14.34 ± 1.12	14.05 ± 1.07	13.98
R.D.	22.24 ± 6.50	27.92 ± 2.06	26.74 ± 2.61	26.29 ± 1.39	26.60 ± 4.29	25.92
R.I.	7.31 ± 4.40	10.94 ± 5.64	11.95 ± 1.53	11.99 ± 0.58	13.00 ± 1.39	10.99
Left lung	45.08 ± 11.26	34.07 ± 3.73	36.07 ± 1.79	36.94 ± 2.48	34.14 ± 3.53	37.32

*Number of animals in parenthesis.

TABLE 6. RELATIVE LOBAR DEPOSITION OF ^{169}Yb LABELLED ALUMINOSILICATE AEROSOLS IN SYRIAN HAMSTERS AT 0-H POST-EXPOSURE. PERCENT OF TOTAL LUNG BURDEN (mean and standard deviation)

	Aerodynamic diameter (μm) D_{ae} (equivalent unit density sphere)					
Lobe	3. 05(6)*	2.09(6)	1.04(6)	0.52(5)	$\leqslant$0.2(6)	Av.(29)
R.A.	17.38 ± 4.22	15.35 ± 5.23	12.76 ± 1.67	13.05 ± 2.32	13.28 ± 1.58	14.41
R.C.	12.33 ± 5.37	12.94 ± 4.78	10.09 ± 3.63	11.96 ± 1.49	8.71 ± 1.96	11.18
R.D.	29.56 ± 10.91	28.43 ± 5.64	30.13 ± 3.95	29.27 ± 4.55	29.39 ± 5.21	29.36
R.I.	9.55 ± 4.17	9.80 ± 3.25	10.66 ± 3.25	11.70 ± 1.46	9.87 ± 3.70	10.27
Left lung	31.17 ± 6.80	34.36 ± 4.75	36.36 ± 5.69	33.96 ± 2.14	38.80 ± 4.18	34.96

* Number of animals in parenthesis.

TABLE 7. RELATIVE LOBAR DEPOSITION OF ^{169}Yb LABELLED ALUMINOSILICATE AEROSOLS IN SYRIAN HAMSTERS AT 20-H POST-EXPOSURE. PERCENT OF TOTAL LUNG BURDEN (mean and standard deviation)

	Aerodynamic diameter (μm) D_{ae} (equivalent unit density sphere)					
Lobe	3.05(4)*	2.09(4)	1.04(4)	0.52(4)	$\leqslant$ 0.2(4)	Av.(20)
R.A.	17.93 ± 5.69	10.82 ± 3.17	14.24 ± 2.51	11.88 ± 1.38	10.51 ± 1.95	13.08
R.C.	17.62 ± 3.48	15.62 ± 2.04	11.52 ± 1.02	12.66 ± 2.33	9.52 ± 1.96	13.39
R.D.	21.75 ± 3.76	23.19 ± 7.02	28.62 ± 2.43	25.26 ± 3.27	27.60 ± 4.19	25.28
R.I.	8.34 ± 1.93	10.24 ± 0.82	10.70 ± 1.93	12.21 ± 2.83	12.26 ± 3.01	10.75
Left lung	34.36 ± 8.10	40.12 ± 10.07	34.90 ± 3.68	38.00 ± 2.01	40.10 ± 7.63	37.50

* Number of animals in parenthesis.

The relative lobar activity percentages at both 0 and 20 h were combined and divided by the appropriate weight percentages of total lung to yield Table 8 for rats and Table 9 for hamsters. The values in these tables are equivalent to relative lobar concentrations of deposited ^{169}Yb labelled particles. In almost every case, the right apical lobe had the highest concentration (except for the case of $\leqslant 0.2$ μm in hamsters). For the remaining lobes, the relative deposition changed with particle size. The relative deposition

TABLE 8. RELATIVE LOBAR CONCENTRATION OF ^{169}Yb LABELLED ALUMINOSILICATE PARTICLES IN BLACK AND WHITE HOODED RATS PERCENT OF TOTAL LUNG BURDEN/PERCENT OF TOTAL LUNG WEIGHT

	D_{ae} (μm)					
Lobe	3.05	2.09	1.04	0.52	$\leqslant$ 0.2	Mean
R.A.	1.21	1.32	1.12	1.05	1.10	1.15
R.C.	0.93	0.95	1.00	1.02	0.97	0.98
R.D.	0.84	0.99	0.96	0.89	0.93	0.92
R.I.	0.75	0.88	0.95	1.02	1.06	0.94
Left lung	1.21	0.97	1.01	1.06	1.01	1.05
Mean	0.99	1.02	1.01	1.01	1.02	1.01
S.D.	0.11	0.09	0.03	0.03	0.03	0.05

TABLE 9. RELATIVE LOBAR CONCENTRATION OF ^{169}Yb LABELLED ALUMINOSILICATE PARTICLES IN FUSED CLAY IN SYRIAN HAMSTERS PERCENT OF TOTAL LUNG BURDEN/PERCENT OF TOTAL LUNG WEIGHT

	D_{ae}(μm)					
Lobe	3.05	2.09	1.04	0.52	$\leqslant$ 0.2	Mean
R.A.	1.60	1.23	1.21	1.14	1.11	1.26
R.C.	1.16	1.13	0.86	0.99	0.73	0.97
R.D.	0.87	0.87	0.97	0.91	0.95	0.91
R.I.	0.78	0.85	0.91	1.02	0.93	0.89
Left lung	0.94	1.06	1.04	1.06	1.14	1.04
Mean	1.07	1.03	1.00	1.02	0.97	1.02
S.D.	0.16	0.08	0.07	0.04	0.08	0.07

concentrations were more uniform among various lobes for smaller particle size (except for the case of $\leqslant 0.2$ μm in hamsters) while the observed variation between lobes tended to be larger for larger particle size.

Morphometry

Replica casts of one rat and one hamster (Table 10) were trimmed and measured using as a basis an idealized model of an airway branch (Fig. 5). The tracheobronchial

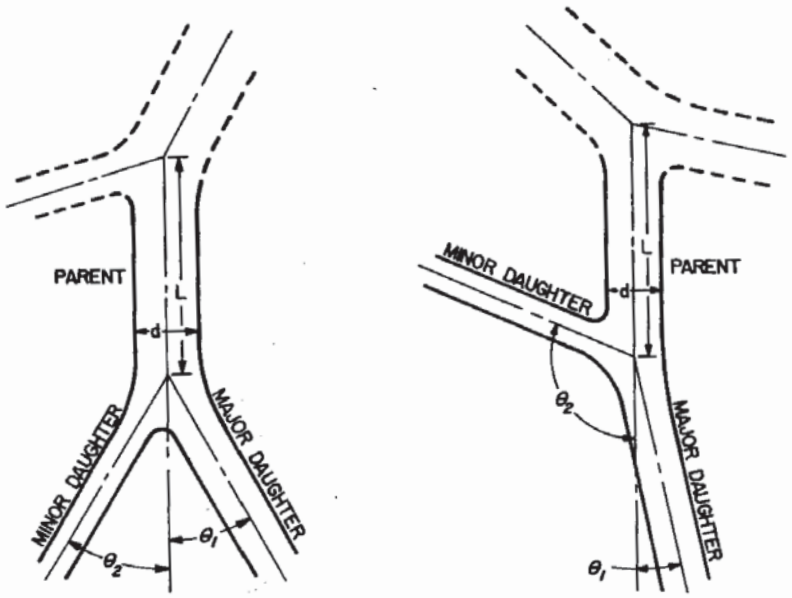

FIG. 5. Idealized model of an airway branch showing the basic morphometric features which were measured on replica casts including the parent tube (airway) diameter, d, the tube length, L, and the branch angles of the major and minor daughters, θ_1 and θ_2.

tree of both species was found to be strongly monopodial in overall structure, in that large, tapering, curved airways with many smaller lateral branches make up the bulk of a trimmed cast. A useful simple model of each lobe of the lungs that can be constructed from the morphometric data is the "typical path model". This model makes use of mean values to provide a single pathway that is a representation of the airways from trachea to respiratory bronchioles. The geometric mean pathway is chosen as the "typical path" since the distribution of divisions to termination tends to approximate a log-normal mathematical function. Tables 11 and 12 summarize the typical paths for rat and hamster. An important feature of the rodent airway is that the mean number of divisions of the bronchial tree between the trachea and first-order respiratory bronchioles varies from lobe to lobe. That is, various lobes have various mean path lengths between trachea and alveoli. More detailed results of the morphometric measurements are shown in Fig. 6. The curves show that "major" bronchial segments (those that make up the long, tapering, slightly curved paths) have increasing branching angles as their diameters decrease. The trend is opposite for "minor" bronchial

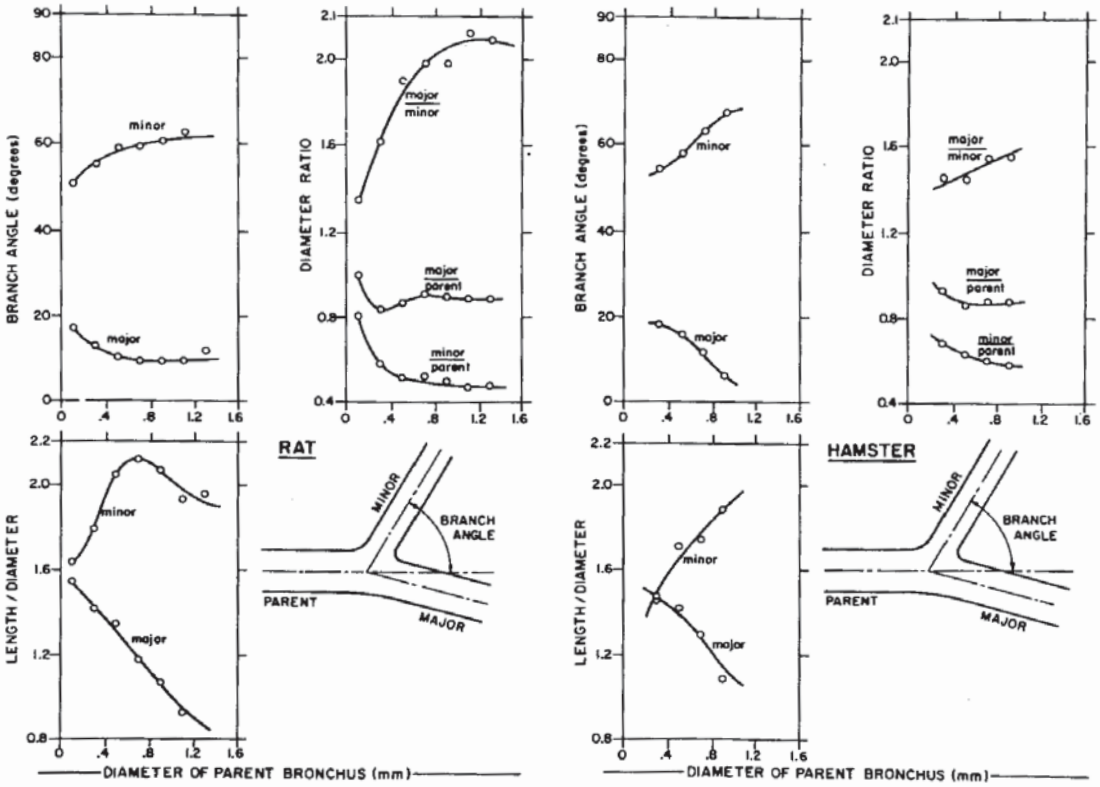

FIG. 6. Comparison of morphometric data illustrating the dependence of tracheobronchial morphology on depth within the lung for rat and Syrian hamster.

segments (those that branch laterally off "major" segments) which causes the overall structure to become more symmetrical at branches deeper within the lung.

TABLE 10. DESCRIPTION OF ANIMALS USED FOR LUNG MORPHOMETRY

Cast number	Animal	Age (months)	Weight (grams)	Sex
HaF–4–73	Syrian hamster	8	143	F
RF –3–72	Hooded rat	12	330	F

DISCUSSION OF RESULTS

For both species pulmonary deposition tended to increase as particle size decreased with 20.7% deposition on the average for rats exposed to the smallest particles; for bronchial deposition a minimum was observed for the 0.52 μm aerodynamic diameter particles with less than 1% on the average of the inhaled aerosol being deposited in the bronchial airways. The total body deposition was found to have a broad minimum for 0.52 μm and 1.04 μm particles with from 14% to 17% total body deposition on the average. A similarly broad minimum was found for naso-pharyngeal deposition for

TABLE 11. TYPICAL PATH MODEL OF AIRWAYS OF RAT FOR EACH LOBE SHOWING SEGMENT LENGTH (L), DIAMETER (d), BRANCH ANGLE (θ_1° CHANGE IN DIRECTION OF BULK AIR FLOW AS SHOWN IN FIG. 5) AND ANGLE TO DIRECTION OF GRAVITY (ϕ°) FOR VARIOUS GENERATION NUMBERS (NO.) STARTING FROM TRACHEA (T)

	R.A.			R.C.			R.I.			R.D.			L.A.			L.D.			
No.	L (mm)	d (mm)	θ_1	L (mm)	d (mm)	θ_1	L (mm)	d (mm)	θ_1	L (mm)	d (mm)	θ_1	L (mm)	d (mm)	θ_1	L (mm)	d (mm)	θ_1	ϕ
T	38	3.4		38	3.4		38	3.4		38	3.4		38	3.4		38	3.4		94
2	4.3	3.0	10	4.3	3.0	10	4.3	3.0	10	4.3	3.0	10	10	2.8	20	10	2.8	20	90
3	3.8	2.0	90	5.4	3.5	5	5.4	3.5	5	5.4	3.5	5	4.0	1.6	70	2.8	3.4	5	85–90
4	1.1	1.6	44	4.8	2.1	65	1.0	3.1	10	1.0	3.1	10	0.85	1.37	26	1.8	3.1	0	50–95
5	2.3	1.1	43	2.44	1.76	32	7.2	2.3	55	3.7	3.1	5	1.69	1.16	17	1.47	2.35	18	57–95
6	0.88	0.94	16	0.70	1.47	8	0.46	1.94	12	1.5	2.9	0	0.94	1.03	18	1.29	2.21	0	39–91
7	0.46	0.87	0	0.93	1.26	12	0.61	1.93	10	2.21	2.76	7	0.69	0.99	6	2.24	1.97	8	74–90
8	1.50	0.81	24	1.88	1.23	3	1.44	1.72	15	0.78	2.67	0	1.27	0.86	22	1.55	1.69	17	61–97
9	0.48	0.66	14	0.69	1.10	9	1.59	1.24	19	1.43	2.28	7	0.92	0.65	27	1.10	1.38	13	
10	0.64	0.60	14	0.74	0.91	21	0.76	1.21	2	1.21	1.95	6	0.71	0.51	18	1.15	1.13	27	
11	0.77	0.46	24	1.13	0.65	25	0.66	1.11	6	1.98	1.70	12	0.60	0.35	28	1.19	0.98	6	
12	0.63	0.36	33	0.60	0.55	13	0.58	1.02	5	1.40	1.74	22				0.89	0.79	21	
13	0.43	0.27	33	0.43	0.44	22	0.70	0.83	9	1.55	1.30	22				0.80	0.59	23	
14				0.52	0.32	25	0.97	0.68	19	1.18	1.12	20				0.57	0.50	30	
15				0.35	0.20	37	0.68	0.46	30	1.14	0.84	24				0.52	0.33	31	
16							0.50	0.34	26	0.81	0.70	19							
17							0.27	0.24	43	0.71	0.53	22							
18										0.53	0.39	23							
19										0.48	0.28	39							
Total	55.3			62.9			65.1			69.3			59.7			65.4			

TABLE 12. TYPICAL PATH MODEL OF AIRWAYS OF HAMSTER FOR EACH LOBE SHOWING SEGMENT LENGTH (L), DIAMETER (d), BRANCH ANGLE (θ_1°) AND ANGLE TO GRAVITY (ϕ°) FOR VARIOUS GENERATION NUMBERS (NO.) STARTING FROM TRACHEA (T)

	R.A.			R.C.			R.I.			R.D.			L.A.			L.D			
No.	L (mm)	d (mm)	θ_1	L (mm)	d (mm)	θ_1	L (mm)	d (mm)	θ_1	L (mm)	d (mm)	θ_1	L (mm)	d (mm)	θ_1	L (mm)	d (mm)	θ_1	ϕ
T	24	2.6		24	2.6		24	2.6		24	2.6		24	2.6		24	2.6		105
2	4.2	2.5	25	4.2	2.5	25	4.2	2.5	25	4.2	2.5	25	8.0	2.3	20	8.0	2.3	20	90
3	4.7	1.8	40	4.5	2.9	15	4.5	2.9	15	4.5	2.9	15	5.1	1.2	60	3.0	2.9	10	80–90
4	0.39	1.53	13	5.4	1.6	60	1.0	3.3	0	1.0	3.3	0	0.72	1.06	33	0.8	2.2	0	25–90
5	1.06	1.25	18	0.1	1.4	0	5.2	2.1	50	2.5	2.5	10	1.54	0.94	6	3.45	2.05	8	30–98
6	1.78	0.88	34	2.5	1.2	25	1.5	1.5	40	2.6	2.1	0	0.94	0.64	36	0.46	1.94	0	
7	0.83	0.68	22	1.08	1.0	19	1.3	1.4	0	2.51	1.86	3	1.04	0.58	27	0.58	1.65	0	
8	0.90	0.59	34	0.66	0.82	6	1.24	1.0	30	0.20	1.74	0	0.82	0.46	41	3.24	1.75	15	
9	0.79	0.43	33	1.21	0.73	12	0.80	0.96	0	0.20	1.70	2	0.58	0.36	18	0.54	1.57	11	
10	0.54	0.38	32	0.97	0.59	11	1.42	0.74	15	2.61	1.41	10	0.26	0.18	64	1.36	1.26	9	
11	0.34	0.27	43	0.81	0.51	18	0.74	0.62	21	1.01	1.18	17				1.64	1.06	18	
12				0.62	0.41	24	0.80	0.53	24	0.63	1.02	10				1.44	0.82	26	
13				0.47	0.31	35	0.57	0.43	16	1.34	0.84	22				0.88	0.62	24	
14							0.65	0.42	6	0.62	0.75	11				0.73	0.49	28	
15							0.51	0.27	39	0.90	0.60	23				0.61	0.38	37	
16										0.79	0.46	25				0.47	0.34	47	
17										0.48	0.39	33							
18										0.43	0.27	40							
Total	39.5			46.5			48.4			50.5			43.0			51.2			

0.52 μm and 1.04 μm particles with from 2% to 4.6% deposition on the average. These results can be explained by the deposition caused by the inertial properties of particles larger than 1 μm and the deposition caused by diffusional properties of the particles smaller than 0.5 μm. The data suggest that inhaled ultrafine particles (about 0.01 μm) may exhibit greater than 20% deposition in the pulmonary region.

For the very small particles the relative lobar deposition tends to be proportional to the lung lobe weight which may be explained as being proportional to the relative aeration of the lobes. However, pulmonary deposition of larger particles appeared to be greater in those lobes having shorter average path lengths from trachea to terminal bronchioles. For example, the typical path from trachea to terminal bronchioles for the right apical lobes of the hamster and rat is shorter than for other right lobes and the relative concentration of 3.05 μm particles deposited in these apical lobes was also greater.

Acknowledgements—Valuable instructions and advice were provided by Mrs Randi Lie Thomas concerning the calibration and operation of the five-port exposure apparatus (THOMAS and LIE, 1963) and concerning animal care and dissections. The authors are indebted for assistance in analysis of morphometric data to Mr G. Michael Schum; for skilled technical assistance to Mr Robert Yarwood, Miss Dolores Esparza and Mrs Donna Duncan; for preparation of illustrations to Mr Emerson Goff; for assistance in data analysis and radiation counting to Mr William Griffith and Mrs Phyllis Peterson and for manuscript preparation to Mrs Judith Miller. This work was supported by the National Institute of Environmental Health Sciences via U.S. Energy Research and Development Administration contract E(29–2)–1013 and conducted in animal-care facilities fully accredited by the American Association for Accreditation of Laboratory Animal Care.

REFERENCES

FUCHS, N. A. and SUTUGIN, A. G. (1966) *Aerosol Science* (edited by DAVIES, C. N.) pp. 1–30. Academic Press Inc., New York.

HOLMA, B. (1968) *Archs envir. Hlth* **17**, 871–873.

KOTRAPPA, P. and LIGHT, M. E. (1972) *Rev. scient. Instrum.* **43**, 1106.

KOTRAPPA, P. and MOSS, O. R. (1971) *Hlth Phys.* **21**, 531–535.

KOTRAPPA, P., WILKINSON, C. J. and BOYD, H. A. (1972) *Hlth Phys.* **22**, 837–843.

MERCER, T. T., TILLERY, M. I. and NEWTON, G. J. (1970) *J. Aerosol Sci.* **1**, 9–15.

MORROW, P. E. and MERCER, T. T. (1964) *Am. ind Hyg. Ass. J.* **25**, 8–14.

NEWTON, G. J., RAABE, O. G., YARWOOD, R. L. and KANAPILLY, G. M. (1976) in *Fine Particles* (Edited by LIU, B. Y. H. Academic Press, N.Y.

PHALEN, R. F., YEH, H. -C., RAABE, O. G. and VELASQUEZ, D. J. (1973) *Anat. Rec.* **177**, 255–264.

RAABE, O. G. (1968) *Am. ind. Hyg. Ass. J.* **29**, 439–443.

RAABE, O. G. (1970) *Inhalation Carcinogenesis* (edited by HANNA, M. G. Jr., NETTESHEIM, P. and GILBERT, J. R.) pp. 123–172. U.S. Atomic Energy Commission Division of Technical Information, Oak Ridge, Tennessee, U.S.A.

RAABE, O. G., BOYD, H. A., KANAPILLY, G. M., WILKINSON, C. J. and NEWTON, G. J. (1975) *Hlth Phys.* **28**, 655–667.

RAABE, O, G., KANAPILLY, G. M. and NEWTON, G. J. (1971) *Inhaled Particles III. Proceedings of an International Syposium organized by the British Occupational Hygiene Society, London, 1970* (edited by WALTON, W. H.) vol. I, pp. 3–17. Unwin Bros., Old Woking, England.

RAABE, O. G. (1975) *Proceedings of the 68th Annual Meeting of the Air Pollution Control Association. Paper No.* 75–50. 3. Air Pollution Control Association, Pittsburgh, Pennsylvania, USA.

STÖBER, W. and FLACHSBART, H. (1969) *Environ. Sci. & Technol.* **3**, 1280–1296.

TASK GROUP ON LUNG DYNAMICS (1966) *Hlth Phys.* **12**, 173–207.

THOMAS, R. G. and LIE, R. (1963) *Procedures and Equipment used in Inhalation Studies on Small Animals.* AEC Research and Development Report, LF–11, Lovelace Foundation, Albuquerque, New Mexico, U.S.A.

THOMAS, R. L. (1969) *Hlth Phys.* **16**, 417–428

DISCUSSION

G. BOULEY: Did you find any significant differences in retention between the sexes at equal body weights? We have observed sexual differences in some microbe infections due to differences in respiratory volume.

Dr RAABE: The variability was very great, so there was no statistically significant difference between the sexes. This may be because there were so few animals involved—five of each sex for each group exposed to each particle size.

D. J. FERIN: How does the deposition in rats and hamsters compare?

Dr RAABE: Again, for the ten animals used for each particle size, the data could not show any statistical difference. In fact, they tend to agree quite well for the two species.

D. J. FERIN: The difference between 0-h and 20-h deposition seems to be small. Can you comment on this?

Dr RAABE: Our definition—an arbitrary one—for bronchial deposition is "those particles which were removed from the lung during a 20-h period after exposure." By comparing the fraction of the total body burden (including the excreta for the 20-h animals) in the lung both for the animals that were sacrificed initially and for those that were maintained for 20 h, we were able to find the fraction of the lung burden which is bronchial deposition; this is given in Table 2. This bronchial clearance was normally small, but for the 2 and 3 μm particles it approaches 40% in the two species. In many individual cases the difference was about 50% for the larger particles, but it was usually less than 10% for the 0.5 μm particles.

W. T. ULMER: Table 3 shows a sharp increase (4.5–17.9% for rats) in the deposition between 1.04 and 2.09 μm dia. particles in the naso-pharynx (skull). What causes this? Could it be conglomeration?

Dr RAABE: We would expect the larger sizes to have greater inertial deposition due to impaction in the small passages of the nose; this probably explains the higher values for the two larger sizes of particles.